hydrology

MDPI

Article

The Impact of Expanding Eucalyptus Plantations on the Hydrology of a Humid Highland Watershed in Ethiopia

Habtamu M. Fenta [1,2,3,*], Tammo S. Steenhuis [1,4], Teshager A. Negatu [1,5], Fasikaw A. Zimale [1], Wim Cornelis [2] and Seifu A. Tilahun [1,6]

[1] Faculty of Civil and Water Resource Engineering, Bahir Dar Institute of Technology, Bahir Dar University, Bahir Dar P.O. Box 26, Ethiopia; tss1@cornnell.edu (T.S.S.); teshager.admasu2019@gmail.com (T.A.N.); fasikaw.atanawbit@bdu.edu.et (F.A.Z.); s.tilahun@cgiar.org (S.A.T.)
[2] Soil Physics Unit, Department of Environment, Ghent University, Campus Coupure Links 653, B-9000 Gent, Belgium; wim.cornelis@ugent.be
[3] Department of Natural Resources Management, University of Gondar, Gondar P.O. Box 196, Ethiopia
[4] Department of Biological and Environmental Engineering, Cornell University, 206 Riley Robb Hall, Ithaca, NY 14853, USA
[5] Abbay Basin Development Office, Bahir Dar P.O. Box 1376, Ethiopia
[6] International Water Management Institute (IWMI), Cantonments, Accra PMB CT 112, Ghana
* Correspondence: habtamumuche.fenta@ugent.be

Abstract: Changes in climate and land use significantly impact downstream water availability. Quantifying these effects in the Ethiopian Highlands is crucial, as 85% of the transboundary water in Egypt and Sudan originates from these highlands. While the impact of climate change on water availability has been widely studied, few experimental studies have examined how it is affected by eucalyptus reforestation. Therefore, the objective was to investigate how eucalyptus expansion impairs water availability in the Ethiopian Highlands. The study was conducted in the 39 km^2 Amen watershed, located in the upper reaches of the Blue Nile. Rainfall data were collected from local agencies from 1990 to 2024, while streamflow data were available only for 2002–2009 and 2015–2018. Actual evapotranspiration was obtained using the WaPOR portal, and land use was derived from Landsat 5 TM and Landsat 8 OLI. The satellite images showed that the eucalyptus acreage increased from 238 ha in 2001 to 799 ha in 2024, or 24 ha y^{-1}. The actual evapotranspiration of eucalyptus was up to 30% greater than that of other land uses during the dry monsoon phase (January to March), resulting in decreased water storage in the watershed over a 23-year period. Since runoff is generated by saturation excess runoff, it takes longer for the valley bottoms to become saturated. In the 2002–2009 period, it took an average of around 160 mm of cumulative effective rain for significant runoff to start, and from 2015 to 2018, 274 mm was needed. Additionally, base flow decreased significantly. The annual runoff trended upward when the annual rainfall was more than the additional amount of water evaporated by eucalyptus, but decreased otherwise.

Keywords: eucalyptus; evapotranspiration; WaPOR evapotranspiration products; discharge; land use change; monsoon climate

check for updates

Academic Editors: Leszek Sobkowiak, Arthur Mynett and David Post

Received: 25 March 2025
Revised: 24 April 2025
Accepted: 9 May 2025
Published: 17 May 2025

Citation: Fenta, H.M.; Steenhuis, T.S.; Negatu, T.A.; Zimale, F.A.; Cornelis, W.; Tilahun, S.A. The Impact of Expanding Eucalyptus Plantations on the Hydrology of a Humid Highland Watershed in Ethiopia. *Hydrology* **2025**, *12*, 121. https://doi.org/10.3390/hydrology12050121

Copyright: © 2025 by the authors. Licensee MDPI, Basel, Switzerland. This article is an open access article distributed under the terms and conditions of the Creative Commons Attribution (CC BY) license (https://creativecommons.org/licenses/by/4.0/).

1. Introduction

With the growing population and resource-intensive economic development, water is becoming scarce in many regions worldwide [1]. Climate change exacerbates water scarcity, particularly in dry areas that are becoming drier, while wet regions are experiencing more rainfall [2,3]. Water scarcity has led to many conflicts, such as, for example, in Yemen [4]

and Sudan [5]. One future conflict can be caused by the Grand Ethiopian Renaissance Dam built by Ethiopia on the border with Sudan [6–8].

Mountainous highlands are the global water towers that provide water to less water-rich regions surrounding them. Globally, in humid areas, as much as 60% of the water originates from highlands, while in semi-arid and arid regions, this can amount to more than 90% [9]. For example, the Ethiopian highlands generate 85% of the water in Egypt and Sudan [7]. These downstream countries are extremely concerned about any changes in the highlands that affect the water supply, and especially the increasing acreage of water-loving eucalyptus trees, which also impact the Grand Ethiopian Renaissance Dam project [7,8].

Smallholder farmers in the Ethiopian Highlands have found that converting their poorest-producing agricultural land into eucalyptus has been financially beneficial. Eucalyptus poles are widely used for building houses and fences, and for scaffolding in construction [10,11]. Farmers also use it to produce charcoal as an energy source [12]. In addition, eucalyptus is used as bio-drainage of saturated land unsuitable for crops [13]. Since their introduction in the Ethiopian Highlands in 1895, *Eucalyptus camaldulensis* and *Eucalyptus globulus* have been planted between 1250 and 2800 m a.s.l. Currently, over 5000 km^2 of its landscape is covered with eucalyptus trees.

However, there are concerns about the potential effects of these eucalyptus plantations on food production, water resources, carbon sequestration, and other ecosystem services [8]. Switching cropland to eucalyptus plantations could reduce wheat and barley production by millions of kilograms, thus affecting the food security of 70,000 to 100,000 households [14]. Eucalyptus trees have higher evapotranspiration rates than other vegetation types due to their distinctive features, which include a high leaf area index, a high density of stomata that remain open for longer periods, and physiological adaptations [15,16]. In Ethiopia, eucalyptus patches significantly enhance evapotranspiration from 3.4 mm d^{-1} to 10 mm d^{-1} in the dry phase [17,18]. Studies in Ethiopia found that 785 L of water was needed to produce one kilogram of eucalyptus biomass [14]. Additionally, eucalyptus' extensive root systems lower the groundwater table during the dry phase [17]. Its impact also reduces runoff by 75% and the drying up of springs and swampy areas [19,20]. Some studies, however, have reported that eucalyptus plantations do not have any significant negative impacts on hydrology [19].

Because previous experimental hydrological studies [18,20] were conducted on areas of 1 km^2 or less, it is uncertain how eucalyptus water use changes the hydrology in the Ethiopian Highlands. Such insight is essential for sustainable water management as it increases and might affect the electricity generated at the Grand Renaissance Dam project and the water security of downstream countries. The rapid growth and large amount of biomass produced by eucalyptus trees may lead to higher water use, highlighting the need to understand its impact. Therefore, to address these concerns and inform sustainable land management strategies, this study examines the effect of expanding eucalyptus plantations on water availability within a monsoon climate watershed in the Ethiopian Highlands. Specifically, the objectives are to (1) quantify the extent of eucalyptus expansion, (2) assess changes in evapotranspiration and streamflow, and (3) assess how land cover change affects the timing of runoff and baseflow reduction.

The study is carried out in the 39 km^2 Amen watershed in the headwaters of the Blue Nile near Lake Tana in the Ethiopian Highlands, where the area of eucalyptus trees has expanded greatly due to its proximity to the rapidly growing town of Bahir Dar. This was possible owing to the availability of calibrated streamflow records at the beginning and near the end of the eucalyptus expansion. Due to the uncertainty of evaluating the water use of eucalyptus at a watershed scale in the experimental studies cited above, we attempt to close the annual water balance of the Amen watershed by augmenting the

measured rainfall and discharge data with satellite-based actual evapotranspiration rates and watershed outflows.

2. Materials and Methods

2.1. Description of the Amen Watershed

The Amen watershed spans an area of 3876 ha in the upper reaches of the Gilgel Abay watershed, which is the main source of water for Lake Tana, contributing roughly 60% of its total inflow [21]. Lake Tana is one of the sources of the Blue Nile, contributing 5% of its total flow. The watershed elevation varies between 2100 and 2434 m a.s.l. (Figure 1). The watershed primarily consists of cultivated land, grasslands, and shrubs. Coinciding with the rapid growth of the nearby town of Bahir Dar, the eucalyptus acreage increased significantly from 2000 onwards. The climate is influenced by the seasonal movement of the Intertropical Convergence Zone (ITCZ) [22]. The region has two distinct seasons: a dry season from October to May and a wet season from June to September. The rain phase contributes 70–90% of annual precipitation [23]. The mean yearly areal rainfall ranges from 1200 to 2100 mm a^{-1}, with most areas receiving between 1600 and 2000 mm a^{-1}. Potential evapotranspiration rates remain the same throughout the year, ranging from around 100 mm per month during the rain phase when it is cloudy to about 120 mm per month in the dry phase with plentiful sunshine (Supplemental Material, Figure S1). Temperatures in the Amen watershed are cooler in the winter, averaging around 16 °C, and warmer during spring and early summer, averaging around 20 °C [24].

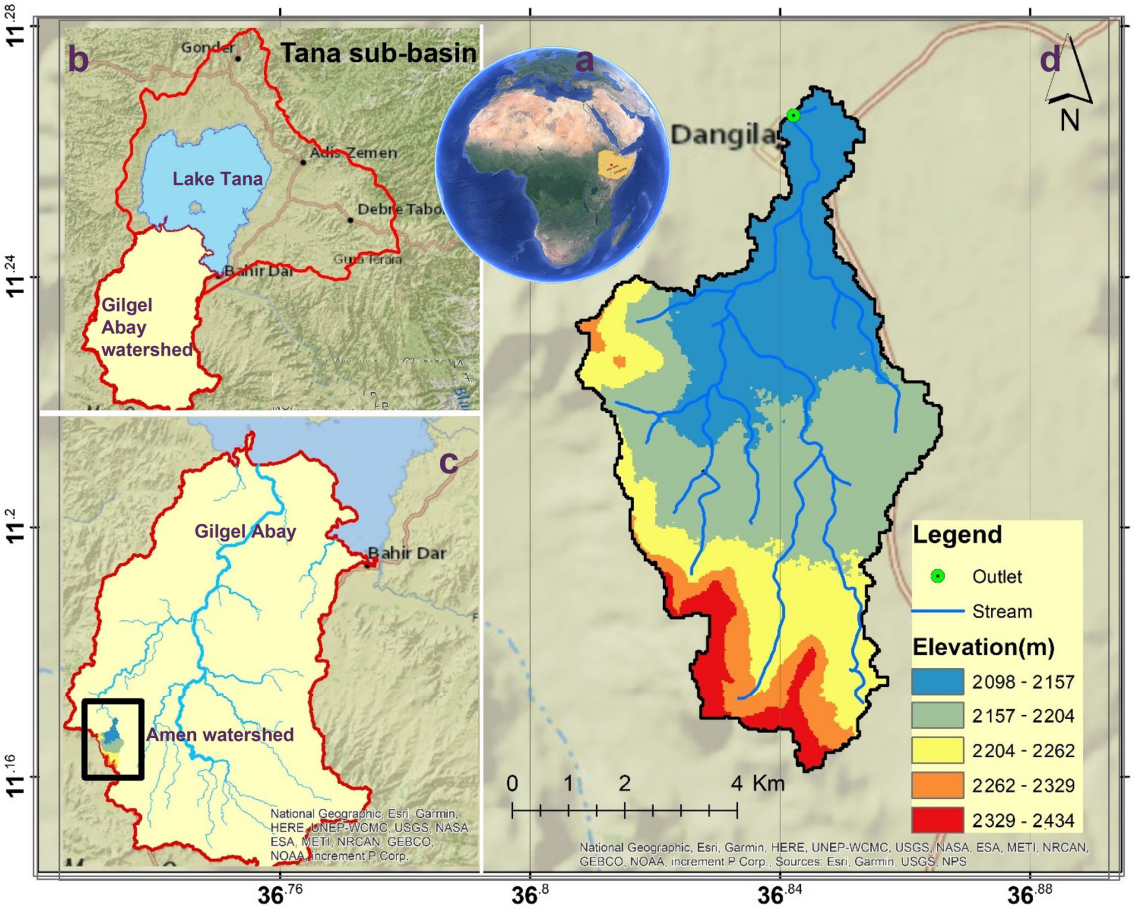


Figure 1. (**a**) Ethiopia (yellow) is located in the horn of Africa; (**b**) the Tana basin with the Gilgel Abay watershed is in the headwaters of the Blue Nile in NW Ethiopia; (**c**) the Gilgel watershed with the Amen watershed (black square) in the southwest; (**d**) the topographical map of the Amen watershed.

Saturation excess is the main storm runoff mechanism. Saturation excess and interflow increase when the watershed wets up after the dry phase. The highest discharge occurs in July and August. Interflow decreases rapidly at the end of the rain phase as storage in the hillslope aquifers decreases. After January, the only water contributing to the stream is from faults.

2.2. Remote Sensing

2.2.1. Land Cover Analysis

Satellite images from Landsat 5 TM and Landsat 8 OLI were collected to analyze land use and cover change for 2001, 2014, and 2024 from the Google Earth Engine (GEE) platform. Landsat 5 provides data from 1984 to 2013 and was used in the 2001 analysis. Landsat 8, launched in 2013, offers higher resolution and was utilized for the 2014 and 2024 land use analyses. Images were selected from January to April with less than 10% cloud coverage. This period minimizes the impact of seasonal variations in vegetation, as crops have been harvested. Additionally, these images have been rectified for atmospheric distortions and georeferenced to the UTM zone 37 N WGS84 coordinate system.

Training data were collected for each land cover type using a combination of methods. These included mean pixel values of the spectral signatures (color information), historical satellite images from Google Earth as reference points to confirm the land cover type in specific locations, and indices like Normalized Difference Built-up Index (NDBI) and Normalized Difference Vegetation Index (NDVI) maps. These indices allow for the accurate identification of built-up areas and eucalyptus plantations. Adequate training sample points were obtained by considering the size of the area of each land cover type and following their proportional pattern, with the same number of samples collected for the years 2001, 2014, and 2024: 160 for cultivated land (36% of the training points), 70 for shrubs (16%), 119 for eucalyptus (27%), 45 for grassland (11%), and 40 for built-up areas (10%). We used the same number of training points across the years to avoid bias towards one class.

We employed the random forest machine learning technique to classify land cover with limited training data. The random forest model was selected because of its extensive application in land use land cover (LULC) change analysis and its proven reliability and accuracy in successfully distinguishing between land cover classes [25,26]. This method is also well-suited for analyzing complex patterns in satellite images, which often contain multiple color bands [27–29]. Similar to [30–32], the watershed images were classified into five land covers: cultivated land, shrubs, eucalyptus, grassland, and built-up areas. A random forest classifier was built for each land cover type, using a default of 100 decision trees. Within the 100 decision trees, the algorithm identified the most effective way to split the data at each decision point by considering the square root of the total number of characteristics [27]. Finally, the data were randomly split into a training set (80%) and a validation set (20%).

2.2.2. Accuracy Assessment

Confusion error matrices were used to measure the accuracy of the classified images. The accuracy metrics used were the Kappa Coefficient, overall accuracy, and producer and user accuracy. The Kappa coefficient measures the agreement between classified data and field sample data, adjusting for chance agreement. Producer accuracy indicates how well the field sample data for each class was classified, while user accuracy reflects the reliability of the classified map from the user's perspective. The accuracy thresholds are defined as follows [31]: 0.81–1 indicates almost perfect agreement, 0.61 to 0.80 significant, 0.41–0.60 moderate, 0.21–0.40 fair, and 0–0.20 slight agreement. Both overall accuracy and the Kappa coefficient demonstrate that the classification results are reliable.

2.3. Hydro-Meteorology

2.3.1. Precipitation

Data on precipitation from 1990 to 2024 were obtained from Ethiopia's National Meteorological Service Agency (NMSA). The Amelia package was utilized to impute values from Addis Kidam station (neighboring weather stations), as the missing values in the precipitation datasets were insignificant, making up less than 10% of the total records [33]. So, the EM convergence was used to control the error and fill in the missing data by parameterizing time in years, neighbouring stations, and priors in RStudio version R-4.4.1. We used the non-parametric Mann–Kendall (MK) test to identify and quantify patterns in precipitation time series data. Sen's slope estimation was also utilized to determine the extent of these trends [34].

2.3.2. Streamflow

Daily stage data at the outlet of the Amen watershed were collected from two government agencies: the Abbay Basin Development Office (ABDO) and the Ministry of Water Resources, Irrigation, and Electricity (MoWIE). The data covered two periods: 2002 to 2009 and 2015 to 2018.

Stage-discharge measurements taken by the agencies were used by [35] to develop rating curves:

$$Q = 1.83(h - ho)^{2.48} \qquad R^2 = 0.91 \tag{1}$$

where Q is the discharge ($m^3\ s^{-1}$), h is the gauge height, and ho is a time-dependent offset to account for scouring or sedimentation at the gauge site:

$$ho = 8.70\ 10^{-5}\ t^3 - 2.75\ 10^{-3}\ t^2 + 0.0137t + 0.1810 \tag{2}$$

where t is the time in years with $t = 1$ in 2002 when the first measurement was taken.

Daily discharge and rainfall data were examined for two distinct periods: 2002–2009 and 2015–2018, to analyze the hydrological response of the Amen watershed. A time series visualization was used to identify the onset and patterns of streamflow in relation to precipitation events. In addition, a linear regression was performed using precipitation and streamflow data from water years (1 April to 31 March) to analyze the relationship between annual precipitation and stream discharge, specifically for the periods of 2002–2009 and 2015–2018.

Like other watersheds in the sub-humid and humid highlands of Ethiopia, saturation excess runoff in the Amen watershed is generated when the valley bottoms become saturated [36]. This phenomenon of saturation excess is common in watersheds throughout the world in the humid and subhumid highlands [36–38], where the infiltration capacity of the surface soil is greater than 80–90% of the rainfall intensities. Therefore, we assessed the change in watershed storage due to the increased eucalyptus acreage by calculating the cumulative effective rain at the beginning of the rain phase to generate discharge. After inspection, the hydrograph showed that after the beginning of the rain phase, the valley bottoms became saturated after 20 mm of cumulative effective precipitation, P_{cum}, had fallen. P_{cum} was computed, starting on June 1:

$$P_{cum} = \sum(P - E_p) \qquad \text{if } P_{cum} \geq 0 \tag{3}$$

$$P_{cum} = 0 \qquad \text{if } \sum(P - E_p) < 0$$

where P is the daily precipitation and E_p is the potential evaporation.

2.3.3. Base Flow

Baseflow is the portion of streamflow sustained between precipitation events, mainly supplied by delayed flow. The potential impact of eucalyptus expansion on base flow was assessed from 2002 to 2009 and from 2015 to 2018 for the dry period months from 1 January to 30 April . To achieve this, the average base flow was calculated for each year to observe the annual trend, and a 14-day average base flow was also calculated for each year to see short-term changes in the study period. A trend analysis using the Mann–Kendall and Sen's slope estimator was employed to identify statistically significant changes in low flows. A paired *t*-test was used to compare the low flow values before and after eucalyptus expansion.

2.3.4. Actual Evapotranspiration (AET)

Many remote sensing products provide actual evapotranspiration data, but often have low spatial resolutions. MODIS has a spatial resolution of 500 m, CMRSET's resolution is 5.6 km, and the resolution of GLEAM is 25 km [32,39]. However, a finer resolution is necessary to differentiate eucalyptus trees from other land uses, as they are often planted on small plots. We therefore selected two actual evapotranspiration products, AET-V2 and AET-V3, which provide actual ET at a 100 m spatial resolution at 10-day intervals (Appendix A, Table A3), allowing us to capture the eucalyptus evapotranspiration [40]. Actual evapotranspiration data for AET-V2 are available from 2009 to 2024, and for AET-V3, from 2018 onwards. These two AET data products can be downloaded from FAO's Water Productivity through Open access to the remotely sensed derived data (WaPOR) portal. The accuracy of WaPOR-derived ET estimates is satisfactory, as indicated by [41,42]. Compared with ground-based measurements, correlation coefficients (R) ranged from 0.71 to 0.97, and Root Mean Square Error (RMSE) values ranged from 0.25 to 1.2 mm d^{-1}. Additionally, eucalyptus is often planted in patches that do not fully cover an area, leading to an underestimation of the evapotranspiration of individual trees.

The AET values between the two versions differed slightly. The difference lies in using improved satellite data inputs, modeling algorithms for arid areas and crop-specific ET behavior, and validation. V3 uses improved remote sensing data, better biophysical parameterization, and separate modeling of soil evaporation and transpiration, enhancing accuracy and spatial consistency. It also includes more extensive ground validation. To ensure continuity between datasets when both datasets were available, we established a linear relationship between AET values from Version 2 and Version 3 for the datasets from 2018 onwards (Supplemental Material, Figure S4). Since both datasets represent the same physical quantity, linear regression provides a simple yet effective method to adjust V2 values to align with V3, ensuring consistency in long-term evapotranspiration analyses. Given the higher quality of AET-V3, as indicated in Table A3, the relationship is used to correct the AET data of Version 2 before 2018 and to generate synthetic AET data for Version 3, thereby facilitating consistency and comparability between the two versions.

3. Results

3.1. Land Use

In the Amen watershed, eucalyptus tree acreage increased significantly (Table 1). In 2001, eucalyptus trees covered 6% of the total land in the watershed. By 2014, this coverage had expanded to 9% and reached 22% in 2024 (Figures 2 and 3). Eucalyptus primarily replaced the shrubland at higher elevations in the southern portion of the watershed (Figure 2). Cropland conversion to eucalyptus plantations mainly occurred near the wet valley bottoms at the outlet, close to the streams, in the northern, lower-lying parts (Supplemental Material, Figure S2). The acreage of shrubs decreased from 12% to 4%, while that

of cropland decreased from 76% to 65% over 23 years (Table 1). Additionally, grassland increased, suggesting that a greater proportion of the valley bottoms became saturated near the middle and end of the rainy phase, making it unsuitable for growing crops [43]. The population increased, resulting in a 1.6% to 3.3% expansion of the built-up area. The overall accuracy for the three observation periods exceeded 80%, the Kappa coefficient was more than 75%, and the producer accuracy was greater than 88% (Table 1).

Table 1. The extent of eucalyptus coverage in hectares, percentage change (2001–2024), and classification accuracy statistics.

Land Use	2001		2014		2024	
	Area (ha)	%	Area (ha)	%	Area (ha)	%
Built-up	62	1.6	75	1.9	127	3.3
Shrubs	457	11.8	398	10.3	142	3.7
Eucalyptus	238	6.1	336	8.7	800	20.7
Grassland	158	4.1	253	6.5	297	7.7
Cultivated	2961	76.4	2813	72.6	2509	64.7
Total	3876	100	3876	100	3876	100
Accuracy statistics						
Overall accuracy		82		84		88
Kappa coefficient		0.75		0.78		0.83
Producer accuracy		88		91		95
User accuracy		84		86		89

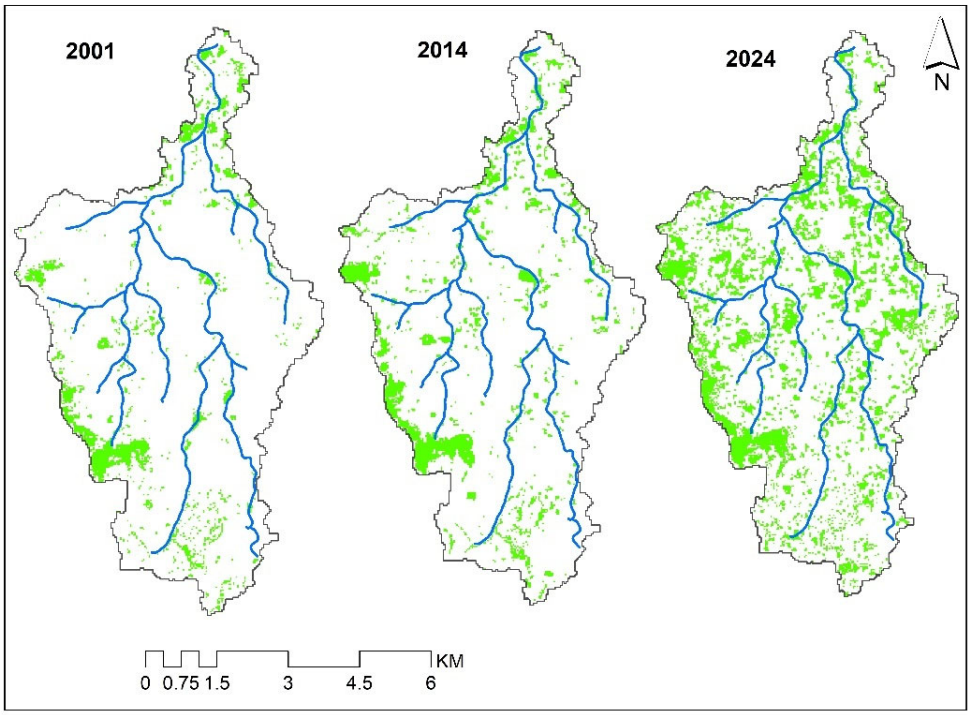


Figure 2. Eucalyptus acreage (shown in green) in 2001, 2014, and 2024 in the Amen watershed. Its spatial expansion highlights the trend over a 23-year period. The blue lines are the streams in the watershed.

The aerial images also showed that the eucalyptus trees were planted in patches throughout the watershed. As an illustration, Figure 3 presents the extent of eucalyptus plantations in the center of the study watershed between April 2005 and April 2021.

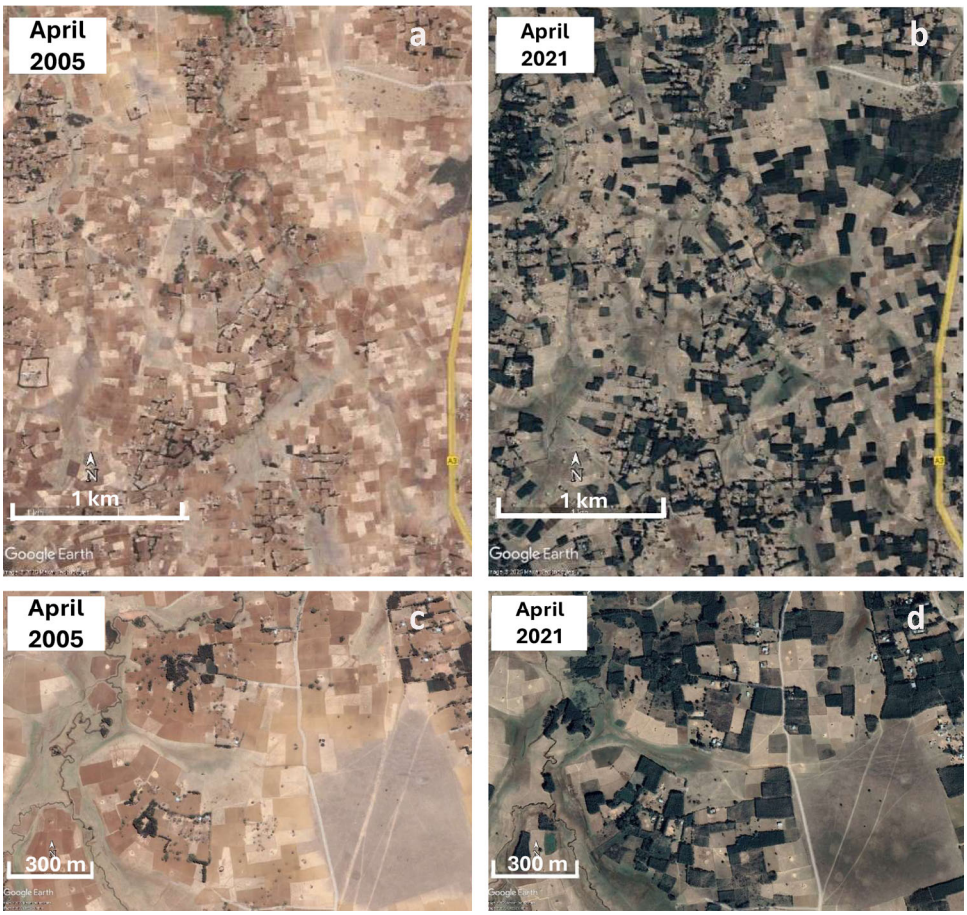


Figure 3. Visual comparison of the extent of eucalyptus plantations in the middle of the study watershed in April 2005 (**a**,**c**) and April 2021 (**b**,**d**), taken from Google Earth Pro satellite imagery.

3.2. Watershed Hydrology

3.2.1. Precipitation

The annual precipitation increased from around 1450 mm a^{-1} in 2001 to 1700 mm a^{-1} in 2024, but the trend was not statistically significant (Appendix A, Table A2, Figure 4). The change in monthly rainfall was inconsistent (Appendix A, Table A2). Long-term rainfall in July and September increased over the 23 years, but in August, it rained less. With an average of 358 mm $month^{-1}$, July saw the largest annual increase with 1.9 mm $month^{-1}$, which was significant ($p = 0.04$). The increase in rainfall during July in the rain phase agrees with the grassland expansion, as shown in Table 1, indicating a greater extent of saturation of the valley bottom lands.

3.2.2. Streamflow

Streamflow is delayed in comparison to when the rainy season begins. Figure 4 depicts the daily discharge at the outlet in yellow of the Amen watershed from 2002 to 2009 and from 2015 to 2018, along with the corresponding rainfall in blue. Streamflow typically begins in early July, while significant rainfall normally starts in May or June. The delay in runoff is due to rainwater initially infiltrating the soil and filling up the pore space from which water was removed by evapotranspiration during the dry phase. Once the valley bottoms are saturated, additional water cannot infiltrate and runs off as overland flow. Once the runoff starts, the overland flow depends mainly on the daily precipitation amounts, with the greatest runoff occurring during events with the highest rainfall amounts.

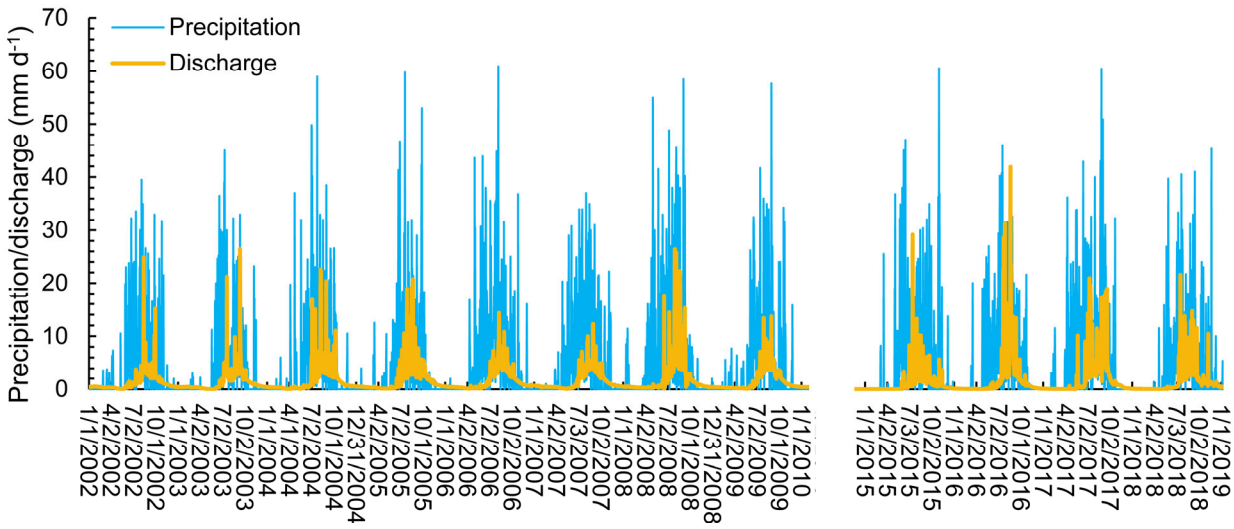


Figure 4. Time series of precipitation and discharge in the Amen watershed for the period when stream discharge records were available (2002–2009 and 2015–2018).

Figure 5 shows annual rainfall and stream discharge, which, on average, increased by 4.9 mm a^{-1} from around 500 mm a^{-1} in 2002 to 600 mm a^{-1} in 2018. The rainfall increased over the same period by 16.4 mm a^{-1} from around 1500 to 1800 mm a^{-1}. In most watersheds that do not undergo a significant change, increasing rainfall will cause a greater increase in runoff because evapotranspiration is at its potential rate when the soil is wet and flows are high. After discussing the delay in runoff in Section 3.2.3, it becomes clear that the greater eucalyptus acreage results in a less-than-expected increase in runoff.

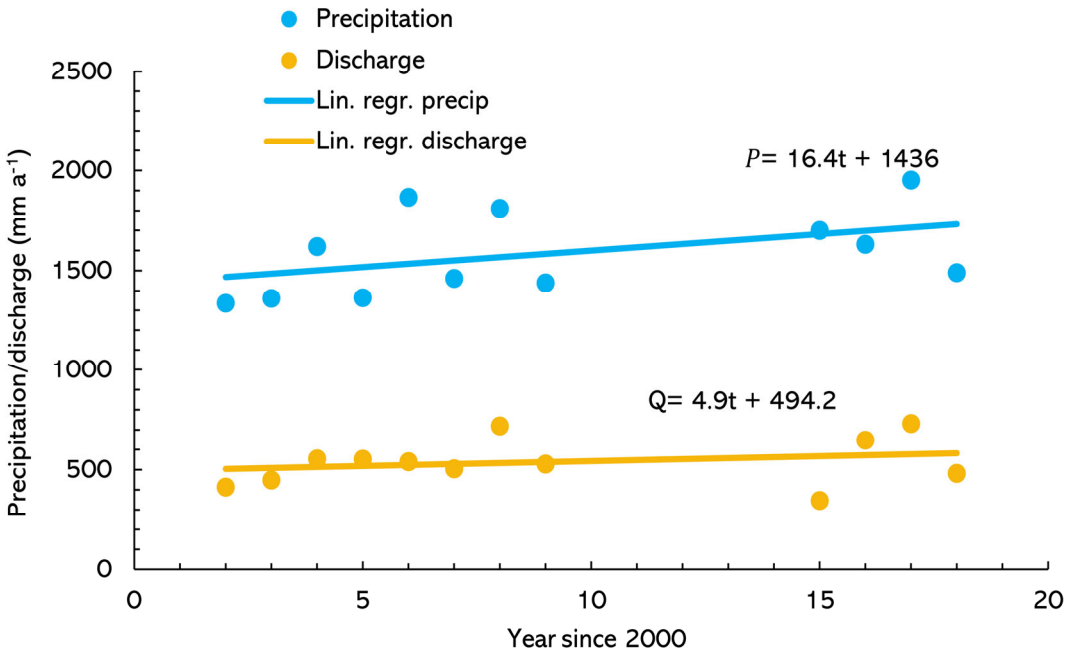


Figure 5. Annual precipitation and discharge of the Amen watershed for water years (1 April to 31 March) for which stream discharge records were available (2002–2009 and 2015–2018). *P* is precipitation in mm a^{-1}; *Q* is discharge in mm a^{-1}; *t* is the number of years since 2000.

3.2.3. Delay in Runoff

In Ethiopian watersheds, saturation excess is the primary runoff mechanism. For significant runoff to occur after the dry phase, the pore space depleted by evapotranspiration

in the dry phase must be replenished [44]. With their extensive root systems, Eucalyptus trees increase evaporation during the dry phase and reduce the amount of water stored. One method for determining the change in water loss through evapotranspiration during the dry phase is to calculate the cumulative effective rain needed to trigger significant runoff at the onset of the rain phase. Effective rain is defined as daily precipitation minus daily potential evapotranspiration (Equation (3)). Upon examining the hydrograph, we observed that after 1 April, the river discharge (including baseflow) increased with each rainfall event when the cumulative daily runoff surpassed 20 mm. At this point, the watershed became hydrologically active, and overland flow from the saturated valley bottom would occur (Figure 6).

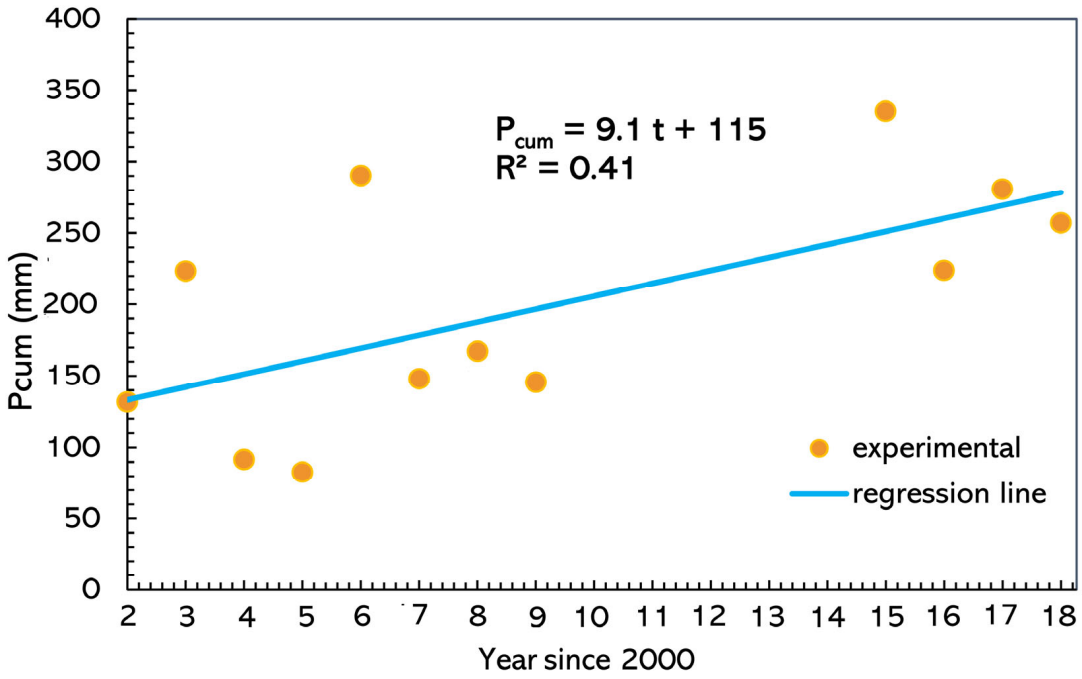


Figure 6. The cumulative effective precipitation, P_{cum}, needed to generate 20 mm of cumulative discharge at the outlet after the beginning of the rain phase for the study periods when discharge data were available (2002–2009 and 2015–2018). Effective rainfall is defined as the amount of precipitation minus the potential evaporation. The time t in the regression equation is the number of years after 2000.

Although the cumulative rainfall before 20 mm of runoff is generated varies considerably in Figure 6, an upward trend is evident (Appendix A, Table A4) in effective rainfall, increasing from an average of 160 mm (2002–2009) to 274 mm (2015–2018). The variation in effective rainfall between years is expected because rainfall was only measured at one location just outside the watershed boundary, and rainfall is spatially highly variable in monsoon climates [37]. For instance, the high effective cumulative rainfall of 290 mm in 2006 before runoff occurred was partly due to two large rainstorms of 75 mm at the beginning of May, which may not have occurred within the watershed. Despite the variability in the data, it suggests a potential shift in the watershed's hydrology, possibly linked to an increase in the eucalyptus area, which extracts greater amounts of water during the dry phase. By extracting more water, eucalyptus decreases the water stored in the watershed, thereby increasing the threshold of rainfall needed to re-saturate soils and initiate runoff.

3.2.4. Base Flow Analysis

Eucalyptus expansion affects dry-season water availability, which is reflected in the baseflow [41,42]. Thus, to investigate the change in storage over time, we can also analyze the discharge at the end of the dry phase, when rainfall is small and does not affect the discharge. The changes in base flow over the years were investigated in several ways. First, we calculated the average discharge at the end of the dry phase between 1 January and 30 April each year. The linear regression analysis (Figure 7a) shows that the yearly average baseflow decreases over time. Second, examining the mean of the 14-day low flow over the four-month periods at the end of the dry phase showed that the 14-day low flow decreased from 0.112 mm d^{-1} in 2002 to 0.015 mm d^{-1} in 2018 (Figure 7b). The decrease in base flow between 2002 and 2009 and between 2015 and 2018 was significant, as indicated by a paired *t*-test ($p < 0.01$). Finally, the base flow duration curves for the Amen watershed, spanning from January 1 to April 30, are presented in the Supplemental Material, Figure S3, for the 2002–2009 and 2015–2018 periods. As expected, they also demonstrate that base flow has decreased significantly. The greatest decrease was in January. These results align with the expansion of eucalyptus plantations shown in Figures 2 and 3 because of their high water uptake during the dry period, which reduces the subsurface watershed storage.

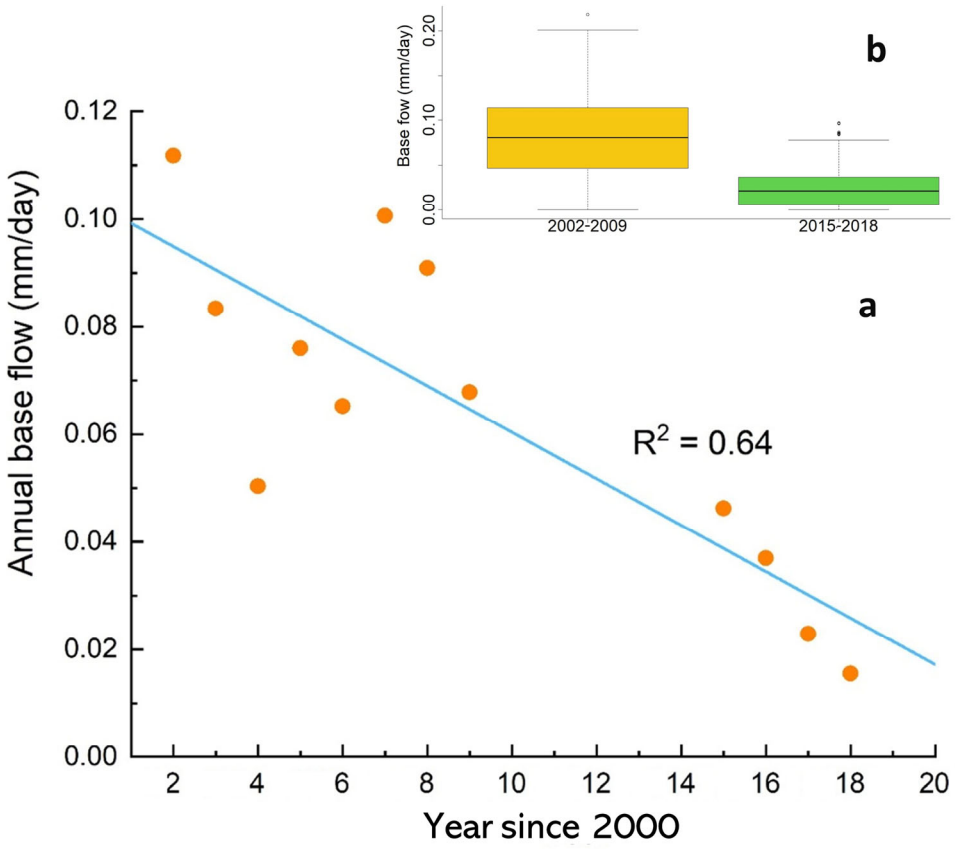


Figure 7. Baseflow during the dry monsoon phase from January 1 to April 30 for the years with stage recordings 2002–2009 and 2015–2018: (**a**) annual average base flow; (**b**) box and whisker plots of daily base flow and a paired *t*-test result.

3.3. Spatial-Temporal Variation of AET

The average yearly evapotranspiration from 2009 to 2024, according to the AET-V2 and AET-V3 datasets, was 929 mm a^{-1} and 850 mm a^{-1}. This compares with an average annual precipitation of 1616 mm a^{-1} over the same period. Both precipitation and actual evapotranspiration increased from 2009 to 2024 (Figure 8). Actual evapotranspiration

increased by 19.6 mm a^{-1} (AET-V2) and 11.7 mm a^{-1} (AET-V3). The annual increase in rainfall was 7.2 mm a^{-1}. Thus, evapotranspiration increased more than precipitation over the same period from 2009 to 2024 (Figure 8). Since the watershed balance should close on an annual basis, we expect that from 2009 to 2024, the streamflow should decrease since the rainfall increase is less than the evaporation. Note, however, that from 2002 to 2018, rainfall increased by 16.4 mm a^{-1} (Figure 5), and over that period, the streamflow increased.

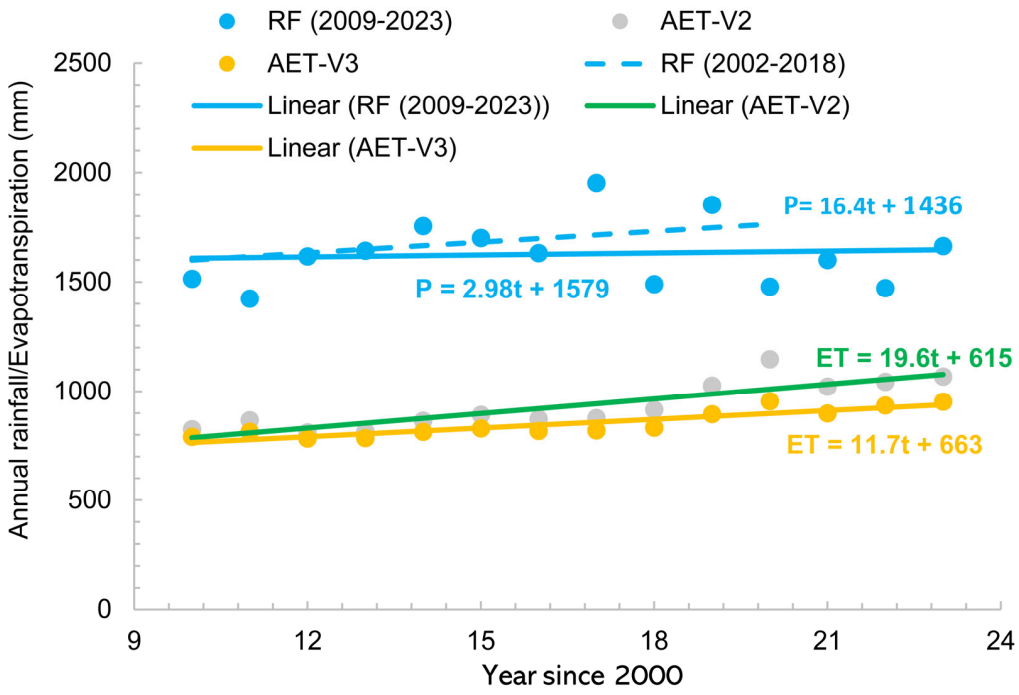


Figure 8. Annual precipitation, *P*, and actual evapotranspiration, ET, of the AET-V2 and AET-V3 evapotranspiration datasets (obtained through the WaPOR portal) from 2009 to 2024. The record of AET-V3 was extended through regression with AET-V2, as both products overlapped from 2018 to 2024. *P* is annual precipitation in mm a^{-1}; ET is annual evapotranspiration in mm a^{-1}; *t* is the year since 2000. RF is rainfall.

Sen's slope and MK-values analysis show that the monthly AET increased over time during most months (Table 2). However, the increase was only significant during the dry months, when moisture was limiting, and the increasing eucalyptus acreage abstracted more water from the soil profile than the vegetation it replaced. During the rain phase, when there is sufficient moisture, evapotranspiration of all vegetation is at the potential rate. Hence, the increasing acreage of eucalyptus will have only a minimal effect on the total watershed evapotranspiration during the rain phase.

The spatial distribution of actual monthly AET during the end of the dry phase (February, March, and April) in the top row of Figure 9 and during the rain phase (July, August, and September) at the bottom of Figure 9 are shown for the years 2009, 2014, and 2024. A different satellite was used in 2024 than in 2009 and 2014. It affected the evaporation measurements. Therefore, the 2009 and 2014 AET data were corrected to ensure continuity in evaporation data. Several trends could be noted. First, the spatial distribution improved with time. The data for 2009 were collected on a 250 by 250 m grid and then downscaled, resulting in the loss of detail. Data for 2014 and 2024 were collected at a 100 m × 100 m scale. Second, despite the difference in input data, it is obvious that AET increased over time, as discussed above (Figure 8). In Figure 9, the shades of color change from predominantly brown to yellow in 2009 to mainly green and dark blue in 2024. Third, AET is significantly less during the dry phase than during the rain phase,

as shown in Table 2. At the end of the rain phase, September has the highest AET of the year, when the soil is still wet, and evapotranspiration is at its potential rate, primarily due to increased incoming solar radiation resulting from fewer clouds compared to previous months. Finally, in July and August 2024, we can clearly distinguish between the saturated river valleys and the hilltops. The valleys have the highest AET rates, and the hilltops, which are drier, have lower AET. In September, the watershed differences in AET with respect to landscape position remain evident, although they are less pronounced.

Table 2. Trend evaluation of monthly actual evapotranspiration in mm month^{-1}, using the AET-V2 and AET-V3 evapotranspiration datasets obtained from the WaPOR portal from 2009 to 2024. AET-V3 was extended through regression analysis with AET-V2 using available data from 2018 to 2024.

Months	Mean ± SD		Slope		Z_{mk}	
	AET-V2	AET-V3	AET-V2	AET-V3	AET-V2	AET-V3
Jan	69 ± 16	65 ± 17 **	2.2	3.2 **	0.37	0.58
Feb	60 ± 11	57 ± 15 *	1.6 *	2.6 *	0.43	0.49
Mar	65 ± 11	62 ± 15 **	1.5 *	2.9 **	0.41	0.66
Apr	58 ± 17	55 ± 17 **	2.0	2.8 **	0.37	0.58
May	73 ± 17	64 ± 15 **	2.5 **	2.3 **	0.52	0.58
Jun	85 ± 13	68 ± 9	1.1	−0.1	0.26	0.03
Jul	69 ± 16	56 ± 8	1.5	0.6	0.26	0.16
Aug	75 ± 14	62 ± 8	1.5	0.8	0.33	0.31
Sep	95 ± 11	77 ± 7	0.9	−0.4	0.2	−0.16
Oct	107 ± 12	90 ± 8	0.3	−0.1	0.07	−0.05
Nov	95 ± 11	82 ± 11	1.5 *	1.6 *	0.41	0.51
Dec	81 ± 14	73 ± 15	2.3 **	2.6 **	0.54	0.54

** Significant at 1% and * significant at 5%.

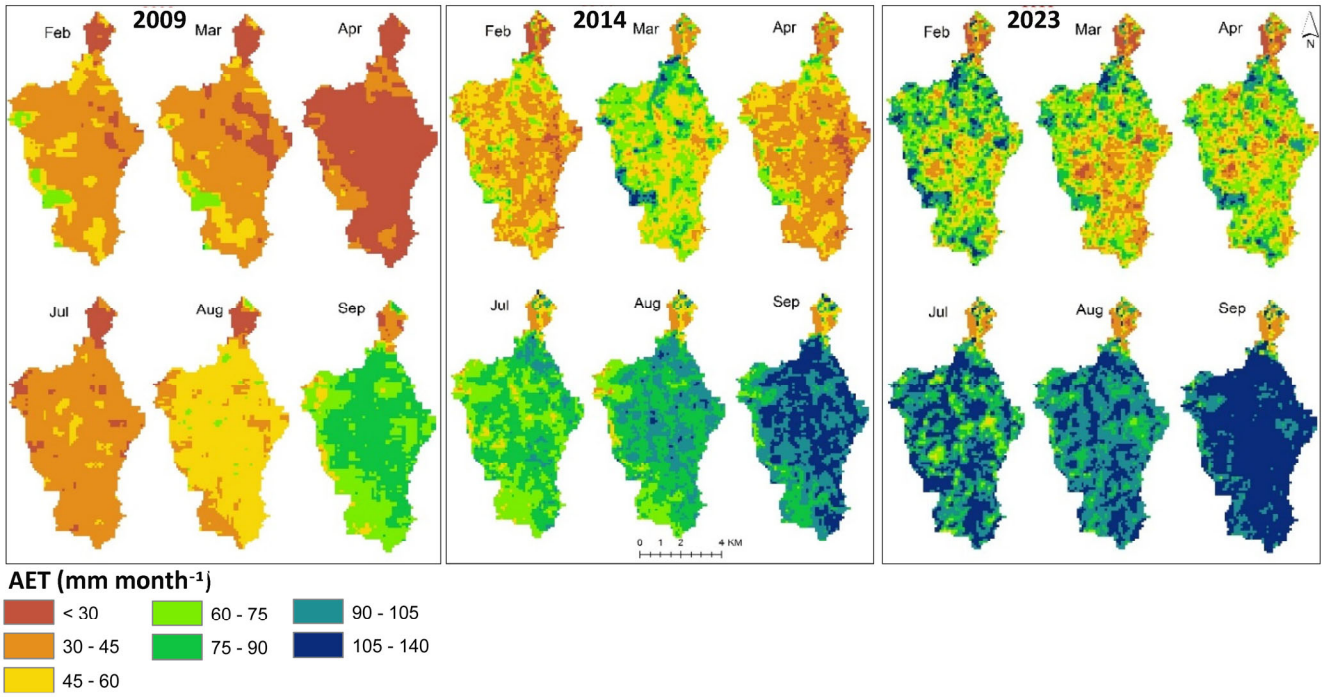


Figure 9. The actual monthly AET-V3 evapotranspiration dataset (obtained through the WaPOR portal) during the dry phase (**upper row**) and rain phase (**bottom row**) months for 2009, 2014, and 2024; the AET-V3 datasets for 2014 and 2009 were obtained from the AET-V2 dataset and corrected for the differences in the two datasets.

3.4. Eucalyptus Response to AET

The analysis highlights significant differences in the temporal AET patterns of various land covers based on WaPOR data, as illustrated in Figure 10. The AET values may be overestimated. However, the main focus should be on the overall trend in AET values rather than the exact numerical values. This means that while the specific figures might be somewhat higher than expected, the general pattern and direction of change in AET over time are more important for understanding the impacts on the watershed.

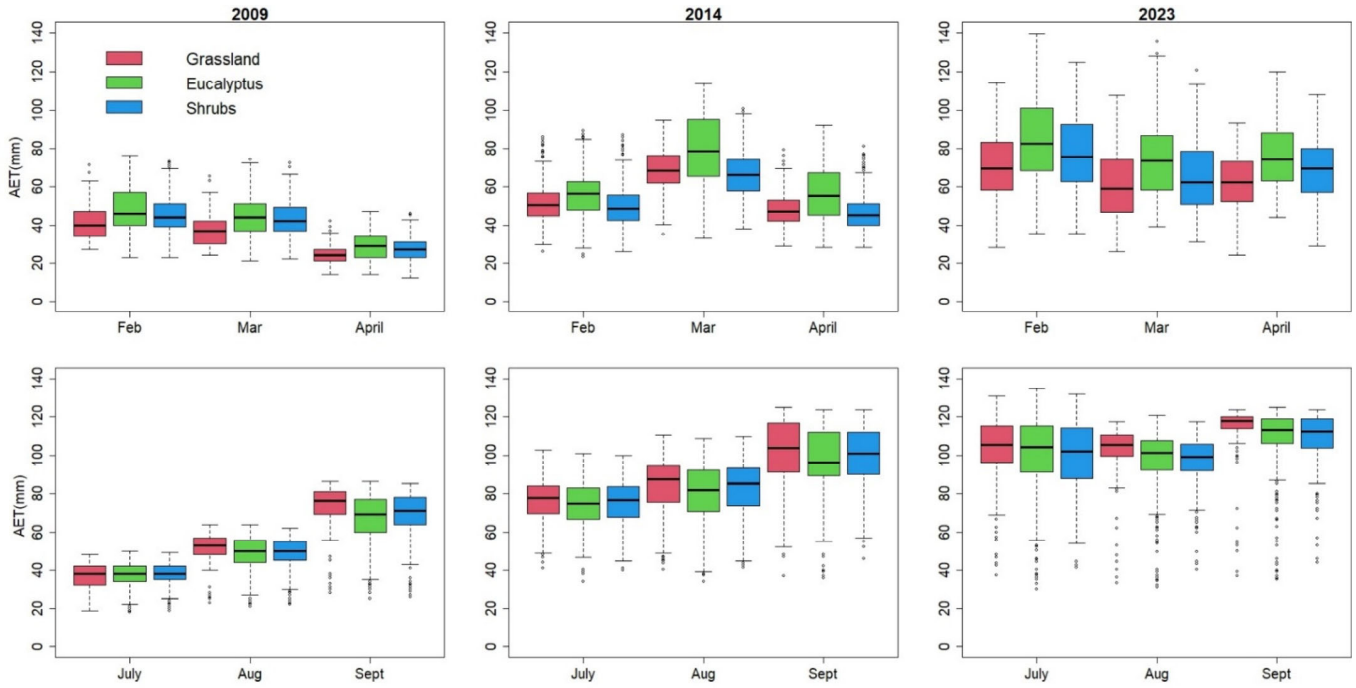


Figure 10. Actual evapotranspiration (AET) in 2009, 2014, and 2024 for the dry (**top row**) and wet (**bottom row**) monsoon phases across diverse land uses within the watershed.

Overall, the trend of land cover responses to AET increased from 2009 to 2024. AET values have increased under eucalyptus, followed by shrubs, across all periods. Grassland AET also increased from 2009 to 2024, particularly in areas near rivers and lower parts of the watershed, where groundwater contributed to the higher AET rates. During the dry season, the average AET from eucalyptus was 10 to 30% greater than from grassland and shrubs.

With their deep root systems and high leaf area indices, eucalyptus trees have a greater capacity for water uptake and transpiration during the dry phase. This characteristic is especially pronounced during the dry phase when the topsoil is dry, but eucalyptus can still access deeper soil moisture. In contrast, grasslands and shrubs, with their shallower root systems and lower leaf area indices, exhibit lower AET rates compared to eucalyptus. This analysis reveals distinct water use patterns among various land uses, particularly eucalyptus, which can significantly impact local hydrology due to its high actual evapotranspiration (AET) rates.

4. Discussion

4.1. Eucalyptus Expansion

Human activities have led to significant changes in the Amen watershed, mainly due to the expansion of eucalyptus plantations (Figure 2 and Table 2), as cultivating eucalyptus is more profitable than growing traditional crops. This change in land-use practice has greatly impacted the hydrology. While annual precipitation increased, baseflow decreased

(Figure 7), and actual evapotranspiration (Figure 8) increased more than the discharge (Figure 5) at the watershed outlet. The latter is due to greater evapotranspiration during the dry phase of eucalyptus trees that have a deeper root system than other trees and can, therefore, access (and dry out) a larger portion of the root zone [14]. This is also why more rain was needed to saturate the valley bottoms, and the start of the saturation excess runoff was delayed (Figure 6). Despite the later start, the annual discharge increased from 2002 to 2018 as rainfall increased more than the actual evaporation over that period (Figure 5). However, from 2009 to 2023, the increase in rainfall was less than the increase in evaporation (Figure 8), and runoff decreased.

4.2. Mass Balance

A water mass balance can check the accuracy of the fluxes using independently measured evapotranspiration, stream discharge, and precipitation data. Mass balances should close on an annual basis when changes in groundwater storage are minimal from year to year due to the steep slopes and long dry periods. However, a major problem in closing the water balance in the Ethiopian Highlands is interflow through faults [45]. Upland watersheds, such as the Amen watershed, typically have positive water balances, with streamflow and evapotranspiration being lower than rainfall because the interflow surfaces downstream as springs.

To verify the mass balance, we analyzed the period from 2000 to 2020, during which eucalyptus acreage increased significantly, and partial streamflow and evapotranspiration records and rainfall measurements were available. Due to missing data for some years, we used the regression in Figure 5 for rainfall and discharge, as well as the actual evapotranspiration in Figure 8, to calculate the terms of the mass balance.

Assuming the entire watershed contributes to the outlet, the mass balance is shown in Figure 11a, Table A4. Obviously, the sum of annual evapotranspiration and discharge is less than precipitation, indicating that a portion of the watershed does not contribute water to the outlet but drains through faults. However, in Figure 11b, the mass balance is nearly closed when assuming 67% of the watershed contributes, particularly when using AET-V3, which applies improved algorithms for evapotranspiration estimation. The latter increases the discharge per unit area (expressed in depth units). The AET-V2 shows a negative mass balance at the beginning of the watershed and a positive water balance in 2020. Thus, AET-V3, which uses more advanced methods to calculate evapotranspiration, is the most accurate.

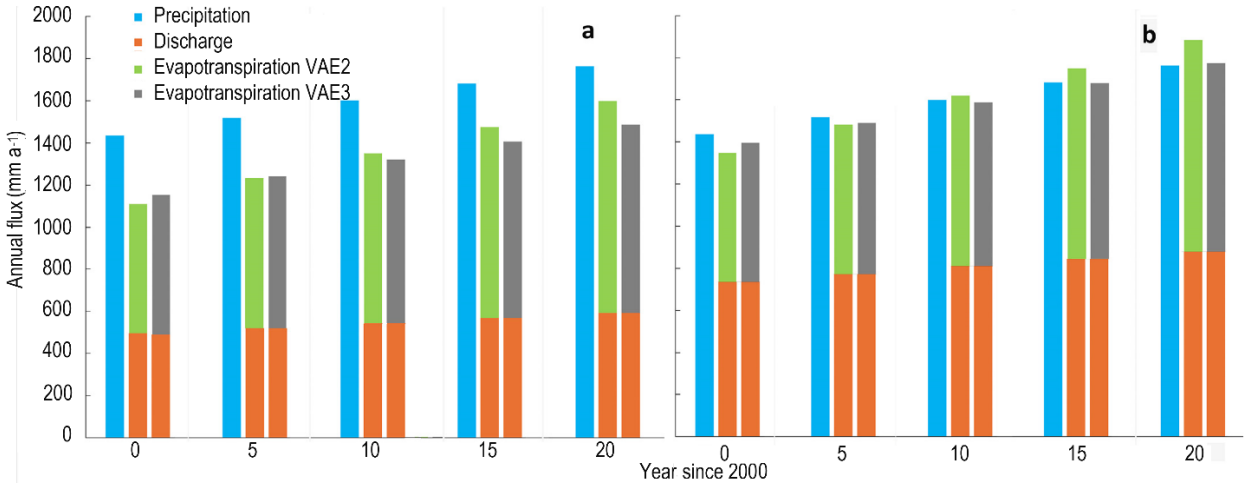


Figure 11. Annual water mass balance for the Amen watershed, 2000–2020: (**a**) the entire watershed contributes to the outlet; (**b**) 67% of the watershed contributes to the outlet.

The expansion of eucalyptus in the Amen watershed appears to increase evapotranspiration during the dry season, resulting in decreased subsurface water storage. As eucalyptus trees consume watershed resources more significantly than other types, there is a hydrological shift characterized by higher rates of evaporation and diminished water availability downstream.

4.3. Comparison with Other Studies and Management Options

Our findings of eucalyptus on the increase in evaporation (Figures 8 and 10), delay in runoff (Figure 6), and less runoff for similar rainfall amounts apply to the shallow and sloping soil profiles in the Ethiopian Highlands. Other studies in sloping watersheds and presumably shallow soils support our findings. Delayed runoff was also observed by [46] in a watershed in South Africa with slopes of 4% and annual rainfall of 1100 mm a^{-1}. Streamflow decreased three years after planting ceased, after nine years of planting. It took five years after harvesting the eucalyptus before the watershed became hydrologically active, and streamflow appeared when the desiccated deep soil water stores were replenished. In another small watershed in South Africa with annual rainfall of nearly 800 mm a^{-1} and a hilly topography and rolling landscapes, both eucalyptus and acacia, after three or more years after planting, reduced streamflow [46]. In central Chile, watersheds with average slopes of 45% and 2500 mm average rainfall, with distinct dry periods, indicate that the removal of eucalyptus plantations increased streamflow, and native forest restoration gradually restored deep soil moisture reservoirs that sustain base flow during dry periods [47]. Similarly, streamflow increases in Uruguay, with a temperate climate without distinct dry periods and rainfall-clearing forests, including eucalyptus [48]. Finally, in a watershed in southern Brazil with average slopes of 7%, streamflow was reduced by mature eucalyptus watersheds [49].

In these sloping watersheds, gravity is the main component of the hydraulic gradient; excess rainfall flows rapidly after the watershed becomes hydraulically active from the hillsides to the valley bottoms, increasing water tables and saturation of the valley bottoms that in turn generate saturated surface runoff [50–52]. Watersheds with eucalyptus take longer to become hydrologically active because more water is evaporated during the dry phase, requiring more rainfall for the watershed to reactivate hydrological processes. Another characteristic of these shallow-sloping watersheds is that a major portion of the excess rainfall is already lost by the end of the rainfall phase [51]. Thus, during the dry phase, plants compete for the small amount of water available, with eucalyptus able to draw from water stores not accessed by other vegetation.

A study showed that forested watersheds with deep soils and permanent groundwater behave differently [53]. This watershed, located on the eastern coast of Brazil, has an annual precipitation of 1150 mm a^{-1}. Since the hydraulic gradient is not gravity-driven, groundwater velocities are much smaller than for perched sloping water tables. Eucalyptus evaporation by cutting down the eucalyptus on the hillside will increase groundwater levels at the site but does not have an immediate response in the valley bottoms because other deep-rooted trees in the watersheds will make up for the loss during the dry phase [54], where, unlike shallow sloping watersheds, groundwater is still available. Similarly, when the eucalyptus trees grow back, other trees will evaporate less. Hence, removing eucalyptus trees will not affect the streamflow in this case.

Finally, an experimental plot study conducted in central Ethiopia [55], found that eucalyptus plantations reduced surface runoff by 21% compared to cultivated land; however, there was no significant difference in runoff between eucalyptus woodlots and grasslands. This contrasts with a study conducted in the Debre Mawi watershed, which has slightly lower annual precipitation, where a 5% increase in eucalyptus cover led to a reduction

in runoff of up to 75%. While plot studies may not always be representative of larger scales [56], this could suggest that replacing cropland with eucalyptus, as was conducted in the Debre Mawi watershed, may reduce streamflow. However, this effect might not occur when eucalyptus replaces other tree species, as was also observed by Davidson [57].

Contrary to our findings, Zerga et al. [19] cited four Ethiopian Highlands publications, indicating that eucalyptus used the same amount of water as acacia and broadleaf species. Three of these studies were presented at an FAO workshop and are unavailable. The fourth publication was by Teshome [58], who cited a study by Davidson [57]. Davidson [57] reported that on a "leakproof hectare" in Nekemet (located halfway between Addis Ababa and the South Sudan border), with an annual rainfall of 2158 mm, eucalyptus and other trees used the same amount of water and did not draw on water reserves, relying solely on rainfall. Davidson did not do any direct measurement. In our study, during the rainy season, when evaporation is less than rainfall, eucalyptus evaporated at the same rate as other trees and crops. Only during the dry season did eucalyptus access water from deeper soil layers compared to other vegetation, and consequently, it had a greater evaporation rate than the cropland it replaced. It is possible that with the relatively short dry phase and high rainfall amounts in Nekemet, the water use is the same. The other possibility is that the "leakproof hectare" assumption is invalid since mass balances of watersheds in the Ethiopian highlands seldom close due to water lost or gained through faults [45].

Thus, while our findings are consistent with those of other sloping watersheds and shallow soils with a climate that has a distinct dry phase, they are different for other watersheds and climates since the type of landscape and climate profoundly impact hydrological behavior and, thus, management implications.

Management options for the highlands with shallow sloping soils are limited since eucalyptus is a source of income for rural families and wood for construction and firewood. Simply prohibiting the growth of eucalyptus on cropland is not an option. Farmers could reduce the eucalyptus acreage and replace it with slower-growing native trees, for payment to downstream users for water saved by not growing the eucalyptus trees. Also, extending the electric grid and replacing charcoal with subsidized electricity for cooking could reduce the demand for wood.

5. Conclusions

This study investigates the impact of converting cultivated land to eucalyptus plantations on water availability in the Amen watershed. Eucalyptus plantations have expanded significantly, growing threefold from 2002 to 2024 and significantly increasing the actual evapotranspiration during the dry period. The watershed hydrology analysis indicated that the annual cumulative discharge increased less than the rise in rainfall, suggesting increased evapotranspiration over the years. It also increased the required cumulative rainfall that generates the early runoff, and we observed a decrease in average base flow and 14-day low flow over time, implying reduced watershed storage at the end of the dry phase. Thus, all four water pathways indicated that more water was removed during the dry phase, and storage within the watershed decreased from 2002 to 2018. This may impact the inflow to the Great Renaissance Dam and, ultimately, the downstream water users, mainly in Sudan and Egypt. To mitigate this, a compensation fee covered by downstream users (Sudan and Egypt) is suggested to encourage farmers to reduce eucalyptus plantations and replace them with trees that use less water during the dry phase. Since the amount of water that can be extracted from watersheds is limited, future research should explore how further eucalyptus expansion will decrease streamflow. Furthermore, research is needed on sustainable eucalyptus management practices that balance economic benefits with water conservation strategies in monsoon climate regions.

Supplementary Materials: The following supporting information can be downloaded at: https://www.mdpi.com/article/10.3390/hydrology12050121/s1, Figure S1: Long-term mean monthly precipitation (P), potential evaporation (PE), and average temperature (Tave) in Amen watershed; Figure S2: Temporal and spatial changes in land use and land cover in the study watershed from 2001 to 2024; Figure S3: The base flow duration curve for the period from 1 January to 30 April for the Amen watershed for the two periods that the discharge data were available: 2002–2009 and 2015–2019; Figure S4: The regression analysis between WaPOR products of actual evapotranspiration (AET) version 2 and 3 from 2018 onwards.

Author Contributions: H.M.F.: conceptualization; formal analysis; investigation, methodology, writing—original draft, and writing—review and editing; W.C., S.A.T. and T.S.S.: conceptualization, formal analysis, methodology; supervision, and writing—review and editing; F.A.Z.: project administration, supervision, and investigation; T.A.N.: data curation and investigation. All authors have read and agreed to the published version of the manuscript.

Funding: This research did not receive any specific grant from funding agencies in the public, commercial, or not-for-profit sectors.

Data Availability Statement: Data will be made available on request.

Acknowledgments: The authors acknowledge the US Geological Survey (USGS) and the FAO for providing access to Landsat and WaPOR ET data. We also appreciate local extension workers for providing essential information about the watershed. Finally, we gratefully acknowledge the International Water Management Institute's Digital Innovations for Water Secure Africa (DIWASA) project funded by the Leona M. and Harry B. Helmsley Charitable Trust.

Conflicts of Interest: The authors declare that they have no known competing financial interests or personal relationships that could have appeared to influence the work reported in this paper.

Appendix A

Table A1. The percentage change detection of land covers in the study watershed (2001–2024).

	2001–2014		2014–2024		2001–2024		
	Area (ha)	%	Area (ha)	%	Area (ha)	%	Rate
Built-up	14	22	51	68	65	105	3
Shrubs	−59	−13	−256	−64	−315	−69	−14
Eucalyptus	97	41	464	138	561	235	24
Grassland	95	61	44	17	1440	89	6
Cultivated	−148	−5	−304	−111	−451	−15	−20

Table A2. Trend analysis of monthly rainfall of the Amen Watershed (1990–2024).

Months	Mean RF (mm)	Monthly Rainy Days	Z_{MK}	Slope	*p*-Value	Difference %
Jan	1	2	−0.78	0.02	0.43	49
Feb	10	2	0.14	0.11	0.89	38
Mar	34	4	−0.57	−0.31	0.57	−30
Apr	46	5	0.34	0.20	0.74	14
May	111	15	−0.37	−0.31	0.71	−9
Jun	233	22	−0.65	−0.73	0.51	−10
Jul	358	24	1.92	2.97	0.05	27
Aug	336	25	−0.97	−0.71	0.33	−7
Sep	237	20	0.45	0.87	0.64	12
Oct	116	15	−0.02	−0.65	0.98	−18
Nov	54	5	0.53	1.14	0.59	70
Dec	9	3	0.39	0.15	0.69	55
Annual	1554	140	0.85	2.74	0.39	5.8

Table A3. Details of the actual evapotranspiration versions 2 and 3 (AET-V2 and AET-V3) datasets are available through the Water Productivity through Open access to the Remotely sensed derived data (WaPOR) portal.

Elements	AET-V2	AET-V3
Data sources and period	MODIS (2009–2013), PROBA-V (2014–current)	PROBA-V and Copernicus Sentinel-2 (2018 onwards)
Resolution	100 m (resampled from 250 m)	100 m
Data type	Decadal (10 days)	Decadal (10 days)
Input layers	NDVI, albedo, fAPAR	NDVI, albedo, fAPAR
AET calculation	Penman–Monteith equation corrected for water stress	Penman–Monteith equation corrected for water stress.

Table A4. Annual precipitation, annual discharge, annual actual evaporation, and the cumulative effective rainfall when the cumulative discharge is greater than 20 mm after the dry phase for periods when discharge data were available (2002–2009 and 2015–2018) for the Amen watershed.

Year	Precipitation mm a^{-1}	Discharge mm a^{-1}	Actual Evap. mm a^{-1}	Cum. Eff. Precip. mm
2002	1337	413	923	132
2003	1361	449	912	224
2004	1620	554	1066	92
2005	1364	553	812	83
2006	1866	540	1326	290
2007	1461	504	957	148
2008	1811	719	1092	167
2009	1439	528	911	146
2015	1701	346	1355	335
2016	1632	647	984	224
2017	1953	731	1222	281
2018	1490	482	1008	257

References

1. UN-Water. *Water Scarcity*; United Nations: New York, NY, USA, 2021.
2. Gosling, S.N.; Arnell, N.W. A global assessment of the impact of climate change on water scarcity. *Clim. Change* **2016**, *134*, 371–385. [CrossRef]
3. Jiménez Cisneros, B.E.; Oki, T.; Arnell, N.W.; Benito, G.; Cogley, J.G.; Doll, P.; Jiang, T.; Mwakalila, S.S. *Freshwater Resources*; Cambridge University Press: Cambridge, UK, 2014.
4. Weiss, M.I. A perfect storm: The causes and consequences of severe water scarcity, institutional breakdown and conflict in Yemen. *Water Int.* **2015**, *40*, 251–272. [CrossRef]
5. Selby, J.; Hoffmann, C. Beyond scarcity: Rethinking water, climate change and conflict in the Sudans. *Glob. Environ. Change* **2014**, *29*, 360–370. [CrossRef]
6. Nasr, H.; Neef, A. Ethiopia's challenge to Egyptian hegemony in the Nile River Basin: The case of the grand Ethiopian Renaissance Dam. *Geopolitics* **2016**, *21*, 969–989. [CrossRef]
7. Gari, Y.; Block, P.; Steenhuis, T.S.; Mekonnen, M.; Assefa, G.; Ephrem, A.K.; Bayissa, Y.; Tilahun, S.A. Developing an approach for equitable and reasonable utilization of international rivers: The Nile River. *Water* **2023**, *15*, 4312. [CrossRef]
8. Abate, D.; Borges, J.G.; Marques, S.; Bushenkov, V. An ecological-economic approach to assess impacts of the expansion of eucalyptus plantations in agroforest landscapes of northern Ethiopia. *Forests* **2022**, *13*, 686. [CrossRef]
9. Messerli, B.; Viviroli, D.; Weingartner, R. Mountains of the world: Water towers for the twenty-first century? In *Managing Water Resources in a Time of Global Change*; Routledge: London, UK, 2009; pp. 27–47.
10. Yirgu, A.; Anjulo, A. First record of *Glycaspis brimblecombei* Moore (hem.: Psyllidae) on Eucalyptus camaldulensis in Ethiopia. *Phytoparasitica* **2019**, *47*, 67–70. [CrossRef]

11. Jaleta, D.; Mbilinyi, B.; Mahoo, H.; Lemenih, M. Eucalyptus expansion as relieving and provocative tree in Ethiopia. *J. Agric. Ecol. Res. Int.* **2016**, *6*, 1–12. [CrossRef]
12. Bekele, M.; Girmay, Z. *Reading Through the Charcoal Industry in Ethiopia: Production, Marketing, Consumption and Impact*; Forum for Social Studies: Addis Ababa, Ethiopia, 2014.
13. Woldemarim, A.; Getachew, T.; Chanie, T. Long-term trends of river flow, sediment yield and crop productivity of Andit Tid watershed, central highland of Ethiopia. *All Earth* **2023**, *35*, 3–15. [CrossRef]
14. Alemneh, T.; Zaitchik, B.F.; Simane, B.; Ambelu, A. Changing patterns of tree cover in a tropical highland region and implications for food, energy, and water resources. *Front. Environ. Sci.* **2019**, *7*, 1. [CrossRef]
15. Farley, K.A.; Jobbágy, E.G.; Jackson, R.B. Effects of afforestation on water yield: A global synthesis with implications for policy. *Glob. Change Biol.* **2005**, *11*, 1565–1576. [CrossRef]
16. Stape, J.L.; Binkley, D.; Ryan, M.G. Eucalyptus production and the supply, use and efficiency of use of water, light and nitrogen across a geographic gradient in Brazil. *For. Ecol. Manag.* **2004**, *193*, 17–31. [CrossRef]
17. Enku, T.; Melesse, A.M.; Ayana, E.K.; Tilahun, S.A.; Abate, M.; Steenhuis, T.S. Groundwater use of a small Eucalyptus patch during the dry monsoon phase. *Biologia* **2020**, *75*, 853–864. [CrossRef]
18. Weldegebriel, L.; Thompson, S.; Tilahun, S.; Guzman, C. Tolerance to waterlogging determines the effectiveness of biodrainage in mitigating runoff in hillslope-scale simulations. *Catena* **2024**, *243*, 108149. [CrossRef]
19. Zerga, B.; Warkineh, B.; Teketay, D.; Woldetsadik, M. The sustainability of reforesting landscapes with exotic species: A case study of eucalypts in Ethiopia. *Sustain. Earth* **2021**, *4*, 5. [CrossRef]
20. Chanie, T.; Collick, A.S.; Adgo, E.; Lehmann, C.J.; Steenhuis, T.S. Eco-hydrological impacts of Eucalyptus in the semi humid Ethiopian Highlands: The Lake Tana Plain. *J. Hydrol. Hydromech.* **2013**, *61*, 21–29. [CrossRef]
21. Alemayehu, T.; McCartney, M.; Kebede, S. The water resource implications of planned development in the Lake Tana catchment, Ethiopia. *Ecohydrol. Hydrobiol.* **2010**, *10*, 211–221. [CrossRef]
22. Conway, D. The climate and hydrology of the Upper Blue Nile River. *Geogr. J.* **2000**, *166*, 49–62. [CrossRef]
23. Abdo, K.; Fiseha, B.; Rientjes, T.; Gieske, A.; Haile, A. Assessment of climate change impacts on the hydrology of Gilgel Abay catchment in Lake Tana basin, Ethiopia. *Hydrol. Process. Int. J.* **2009**, *23*, 3661–3669. [CrossRef]
24. Wale, A.; Rientjes, T.; Dost, R.; Gieske, A. *Hydrological Balance of Lake Tana Upper Blue Nile Basin, Ethiopia*; ITC: Enschede, The Netherlands, 2008.
25. Breiman, L. Random forests. *Mach. Learn.* **2001**, *45*, 5–32. [CrossRef]
26. Rodriguez-Galiano, V.F.; Ghimire, B.; Rogan, J.; Chica-Olmo, M.; Rigol-Sanchez, J.P. An assessment of the effectiveness of a random forest classifier for land-cover classification. *ISPRS J. Photogramm. Remote Sens.* **2012**, *67*, 93–104. [CrossRef]
27. Oshiro, T.M.; Perez, P.S.; Baranauskas, J.A. How many trees in a random forest? In Proceedings of the Machine Learning and Data Mining in Pattern Recognition: 8th International Conference, MLDM 2012, Berlin, Germany, 13–20 July 2012; pp. 154–168.
28. Gizachew, B.; Solberg, S.; Næsset, E.; Gobakken, T.; Bollandsås, O.M.; Breidenbach, J.; Zahabu, E.; Mauya, E.W. Mapping and estimating the total living biomass and carbon in low-biomass woodlands using Landsat 8 CDR data. *Carbon Balance Manag.* **2016**, *11*, 13. [CrossRef]
29. Belgiu, M.; Csillik, O. Sentinel-2 cropland mapping using pixel-based and object-based time-weighted dynamic time warping analysis. *Remote Sens. Environ.* **2018**, *204*, 509–523. [CrossRef]
30. Eshetie, A.A.; Wubneh, M.A.; Kifelew, M.S.; Alemu, M.G. Application of artificial neural network (ANN) for investigation of the impact of past and future land use–land cover change on streamflow in the Upper Gilgel Abay watershed, Abay Basin, Ethiopia. *Appl. Water Sci.* **2023**, *13*, 209. [CrossRef]
31. Landis, J.R.; Koch, G.G. An application of hierarchical kappa-type statistics in the assessment of majority agreement among multiple observers. *Biometrics* **1977**, *33*, 363–374. [CrossRef]
32. Miralles, D.G.; Holmes, T.; De Jeu, R.; Gash, J.; Meesters, A.; Dolman, A. Global land-surface evaporation estimated from satellite-based observations. *Hydrol. Earth Syst. Sci.* **2011**, *15*, 453–469. [CrossRef]
33. Honaker, J.; King, G.; Blackwell, M. Amelia II: A program for missing data. *J. Stat. Softw.* **2011**, *45*, 1–47. [CrossRef]
34. Sen, P.K. Estimates of the regression coefficient based on Kendall's tau. *J. Am. Stat. Assoc.* **1968**, *63*, 1379–1389. [CrossRef]
35. Negatu, T.A.; Zimale, F.A.; Steenhuis, T.S. Establishing Stage–Discharge Rating Curves in Developing Countries: Lake Tana Basin, Ethiopia. *Hydrology* **2022**, *9*, 13. [CrossRef]
36. Tilahun, S.A.; Ayana, E.K.; Guzman, C.D.; Dagnew, D.C.; Zegeye, A.D.; Tebebu, T.Y.; Yitaferu, B.; Steenhuis, T.S. Revisiting storm runoff processes in the upper Blue Nile basin: The Debre Mawi watershed. *Catena* **2016**, *143*, 47–56. [CrossRef]
37. Bayabil, H.K.; Tilahun, S.A.; Collick, A.S.; Yitaferu, B.; Steenhuis, T.S. Are runoff processes ecologically or topographically driven in the (sub) humid Ethiopian highlands? The case of the Maybar watershed. *Ecohydrology* **2010**, *3*, 457–466. [CrossRef]
38. Mhiret, D.A.; Dersseh, M.G.; Guzman, C.D.; Dagnew, D.C.; Abebe, W.B.; Zimale, F.A.; Zaitchik, B.F.; Tilahun, S.A.; Walraevens, K.; Steenhuis, T.S. Topography impacts hydrology in the sub-humid Ethiopian Highlands. *Water* **2022**, *14*, 196. [CrossRef]

39. Guerschman, J.P.; McVicar, T.R.; Vleeshower, J.; Van Niel, T.G.; Peña-Arancibia, J.L.; Chen, Y. Estimating actual evapotranspiration at field-to-continent scales by calibrating the CMRSET algorithm with MODIS, VIIRS, Landsat and Sentinel-2 data. *J. Hydrol.* **2022**, *605*, 127318. [CrossRef]
40. Blatchford, M.L.; Mannaerts, C.M.; Njuki, S.M.; Nouri, H.; Zeng, Y.; Pelgrum, H.; Wonink, S.; Karimi, P. Evaluation of WaPOR V2 evapotranspiration products across Africa. *Hydrol. Process.* **2020**, *34*, 3200–3221. [CrossRef]
41. Smakhtin, V.U. Low flow hydrology: A review. *J. Hydrol.* **2001**, *240*, 147–186. [CrossRef]
42. Buttle, J.M. Mediating stream baseflow response to climate change: The role of basin storage. *Hydrol. Process.* **2018**, *32*, 363–378. [CrossRef]
43. Lemenih, M.; Kassa, H. Re-greening Ethiopia: History, challenges and lessons. *Forests* **2014**, *5*, 1896–1909. [CrossRef]
44. Steenhuis, T.S.; Alemie, T.C.; Muche, H.; Tilahun, S.A.; Zimale, F.A.; Mhiret, D.A. Effect of eucalyptus on blue and green water availability and discharge in the tropical highlands: An interpretation of available literature. *J. Hydrol. Hydromech.* **2023**, *71*, 221–230. [CrossRef]
45. Adem, A.A.; Addis, G.G.; Aynalem, D.W.; Tilahun, S.A.; Mekuria, W.; Azeze, M.; Steenhuis, T.S. Hydrogeology of volcanic highlands affects prioritization of land management practices. *Water* **2020**, *12*, 2702. [CrossRef]
46. Kaptein, N.D.; Clulow, A.D.; Everson, C.S.; Toucher, M.L.; Germishuizen, I. The influence of different tree species and age on the surface water balance of a small commercial forestry catchment. *J. Hydrol. Reg. Stud.* **2024**, *54*, 101893. [CrossRef]
47. Lara, A.; Jones, J.; Little, C.; Vergara, N. Streamflow response to native forest restoration in former Eucalyptus plantations in south central Chile. *Hydrol. Process.* **2021**, *35*, e14270. [CrossRef]
48. Alonso, J.; Silveira, L.; Vervoort, R.W. Assessing effects of afforestation on streamflow in Uruguay: From small to large basins. *Hydrol. Process.* **2024**, *38*, e15272. [CrossRef]
49. Ferreto, D.O.C.; Reichert, J.M.; Cavalcante, R.B.L.; Srinivasan, R. Water budget fluxes in catchments under grassland and Eucalyptus plantations of different ages. *Can. J. For. Res.* **2021**, *51*, 513–523. [CrossRef]
50. Alemie, T.C.; Tilahun, S.A.; Ochoa-Tocachi, B.F.; Schmitter, P.; Buytaert, W.; Parlange, J.Y.; Steenhuis, T.S. Predicting shallow groundwater tables for sloping highland aquifers. *Water Resour. Res.* **2019**, *55*, 11088–11100. [CrossRef]
51. Tilahun, S.A.; Yilak, D.L.; Schmitter, P.; Zimale, F.A.; Langan, S.; Barron, J.; Parlange, J.Y.; Steenhuis, T.S. Establishing irrigation potential of a hillside aquifer in the African highlands. *Hydrol. Process.* **2020**, *34*, 1741–1753. [CrossRef]
52. Addisie, M.B.; Ayele, G.K.; Hailu, N.; Langendoen, E.J.; Tilahun, S.A.; Schmitter, P.; Parlange, J.-Y.; Steenhuis, T.S. Connecting hillslope and runoff generation processes in the Ethiopian Highlands: The Ene-Chilala watershed. *J. Hydrol. Hydromech.* **2020**, *68*, 313–327. [CrossRef]
53. Smethurst, P.J.; Almeida, A.C.; Loos, R.A. Stream flow unaffected by Eucalyptus plantation harvesting implicates water use by the native forest streamside reserve. *J. Hydrol. Reg. Stud.* **2015**, *3*, 187–198. [CrossRef]
54. Smethurst, P.J.; Petrone, K.C.; Langergraber, G.; Baillie, C.C.; Worledge, D.; Nash, D. Nitrate dynamics in a rural headwater catchment: Measurements and modelling. *Hydrol. Process.* **2014**, *28*, 1820–1834. [CrossRef]
55. Jaleta, D.; Mbilinyi, B.P.; Mahoo, H.F.; Lemenih, M. Effect of Eucalyptus expansion on surface runoff in the central highlands of Ethiopia. *Ecol. Process.* **2017**, *6*, 1. [CrossRef]
56. Fenta, H.M.; Aynalem, D.W.; Malmquist, L.; Haileslassie, A.; Tilahun, S.A.; Barron, J.; Adem, A.A.; Adimassu, Z.; Zimale, F.A.; Steenhuis, T.S. A critical analysis of soil (and water) conservation practices in the Ethiopian Highlands: Implications for future research and modeling. *Catena* **2024**, *234*, 107539. [CrossRef]
57. Davidson, J. *The Eucalypt Dilemma: Arguments for and Against Eucalypt Planning in Ethiopia*; The Forestry Research Centre Seminar Note Series No. 1. A. A. Forestry Research Center: Addis Abeba, Ethiopia, 1989.
58. Teshome, T. Is Eucalyptus ecologically hazardous tree species? *Ethiop. e-J. Res. Innov. Foresight (Ee-JRIF)* **2009**, *1*, 128–134.

Disclaimer/Publisher's Note: The statements, opinions and data contained in all publications are solely those of the individual author(s) and contributor(s) and not of MDPI and/or the editor(s). MDPI and/or the editor(s) disclaim responsibility for any injury to people or property resulting from any ideas, methods, instructions or products referred to in the content.